Time-of-Flight Characterization of a Microfabricated Electrospray Thruster Emitter Array

IEPC-2017-148

Presented at the 35th International Electric Propulsion Conference
Georgia Institute of Technology • Atlanta, Georgia • USA
October 8 – 12, 2017

E. Grustan-Gutierrez [1] and M. Gamero-Castaño.[2]
University of California, Irvine, California 92717, USA

Abstract: **Electrospray thrusters can deliver the efficient primary propulsion and attitude control actuation needed by small satellites. The microfabricated multiemitter array is an ideal implementation of this technology because it addresses the thrust, volume, mass and scalability requirements across the size range of smallsats. This article describes the characterization of an internally fed, 64 emitter microfabricated array. The characterization is based on the use of the time-of-flight technique to indirectly measure the thrust and the mass flow rate of the beam. The electrospray source features an emitter and an extractor electrodes, etched on silicon; and an etched glass wafer which, bonded to the back side of the emitter electrode, provides space for a reservoir from which the propellant is distributed to the emitters. The three wafers are bonded into a single component. The main novelty of this electrospray source is the use of individual flow-restrictive channels, etched on the back of the emitter wafer, and connecting each emitter to the common distribution reservoir. This construction decouples the design and fabrication of the emitters from the need to provide a flow path with sufficient hydraulic resistance for each emitter.**

Nomenclature

I_E	=	emitter current
I_{sp}	=	specific impulse
m	=	droplet mass
$\dot{m}_{TOF}$	=	mass flow rate measured with the time-of-flight technique
Q	=	volumetric flow rate
Q_{FM}	=	dimensionless flow rate
q	=	droplet charge
T_{TOF}	=	thrust measured with the time-of-flight technique
v	=	droplet velocity
V_A	=	acceleration voltage
V_E	=	emitter voltage
ΔP	=	pressure of the propellant at reservoir
ϕ_L	=	voltage loss along the cone-jet
η_p	=	propulsive efficiency

[1] Postdoctoral Researcher, Department of Mechanical and Aerospace Engineering, enric.grustan@qmul.ac.uk.
[2] Associate Professor, Department of Mechanical and Aerospace Engineering, mgameroc@uci.edu.

I. Introduction

ELECTROSPRAY propulsion atomizes a liquid propellant into charged droplets and ions using the electrospraying technique. The usefulness of this ionization technique for electric propulsion was first recognized in the 60's,[1] and interest resurfaced in the late 90's with the arrival of smallsats and the need for efficient micropropulsion.[2,3] Individual electrospray emitters operate in the milli-Watt and micro-Newton range, and at relatively high specific impulse. The efficiency for electrical-to-jet power conversion is remarkably high at low power levels (above 70% at 1 mW),[4] and remains constant at increasing power. The high efficiency is a consequence of the processes associated with the atomization and charging of the propellant: the atomization requires a small viscous dissipation,[5] and does not require the formation of a plasma.

A typical electrospray emitter cross section has a diameter of 100 microns. Since the atomization, charging and acceleration of the propellant only requires the use of an electrostatic field, the area occupied by an emitter can be made to approach this small 0.01 mm^2 area without penalizing performance. Most propulsion applications require thrust levels considerably larger than one micro-Newton, and electrospray propulsion can achieve this by multiplexing a large number of emission sites. This multiplexing has been implemented in several ways;[6,7] in this study we use micromachining techniques to fabricate a regular array of emitters.

Micromachined arrays can be divided in two types depending on how the propellant is delivered to the emission sites. In externally fed arrays each emitter is a solid and slender protrusion raising from a common plane, and the propellant reaches its tip by capillary wetting of the surface or through a porous media.[8,9] Once the propellant wets the emission sites, the electrostatic pull at the tips drives the flow in steady state operation. The second type is the internally fed array, which is the one considered in this article: the emitters are tubes typically etched on silicon, connected to and fed from a common and sealed manifold etched on the back of the wafer, and the flow of propellant is driven by an imposed pressure drop. Since the propellant is always encased by solid walls except at the emitter tip, internally fed arrays are less susceptible to electric shorting by propellant bridging of the emitter and extractor electrodes, a life-limiting mechanism in these structures characterized by narrow gaps of hundreds of microns between electrodes. Minimizing differences of hydraulic resistances among emitters is especially important in internally fed arrays, because the flow rate in each emitter is inversely proportional to its hydraulic resistance (the pressure in the manifold is common to all emitters), and a uniform flow distribution among emitters is key for correct operation. Furthermore, the pressure in the manifold must be relatively large, at least a few times larger than both the capillary pressure at the liquid meniscus interface and the vapor pressure of impurities in the propellant, to eliminate flow variations among emitters and disturbances caused by the formation of bubbles. For typical propellants, flow rates, and tube lengths (a few hundred microns, limited by wafer thicknesses and aspect ratios of the deep reactive ion etching DRIE equipment used to fabricate them), a tube diameter D of a few microns is required to provide the needed pressure drop between the manifold and the emitter tip. However, these small diameters are impractical due to limitations on the aspect ratio of DRIE equipment and, being near fabrication tolerances, to variations on the flow rate between emitters (the hydraulic resistance scales with D^{-4}). To address this problem Shea and colleagues have developed a process based on the insertion of microbeads in the emitters' channels to arbitrarily increase the hydraulic resistance of the emitters.[10,11] This technique does not guarantee a uniform filling of the emitters,[12] nor that the beads remain in place throughout the lifespan of the thruster.[13] In some of their latest prototypes, Shea et al. have increased the hydraulic resistance by reducing the inner diameter of the emitter,[14] but this ties the geometry and fabrication of the emitter to the hydraulic resistance requirement.

The micromachined array described and tested in this article is internally fed. An important novelty is the decoupling of the required hydraulic resistance from the geometry and fabrication of the tubular emitters. We do this by etching a channel for each emitter in the back side of the wafer, linking the emitter with the common manifold. The cross section and length of these channels provide the desired hydraulic resistance for each emitter. This solution allows making flow-resistive channels orders of magnitude longer than the emitter column (e.g. tens of millimeters versus one hundred microns), with a cross section of aspect ratio near one. The etching of these channels is much simpler than that of the inner channel of a standing emitter with the small diameter needed to provide a similar hydraulic resistance.

II. Electrospray Source Description and Testing

A. Source Description and Fabrication

Ref. [15] provides a detailed description of the microfabrication recipe. The emitters are etched on a 450 μm thick Si wafer and arranged in a square 8x8 array with a pitch of 1 mm. Each emitter is a tube with an external diameter of

90 μm, an inner diameter of 40 μm, a height of 300 μm, and is located inside a well 300 μm deep and 0.9 mm in diameter. The channels etched on the back side of the wafer for increasing the hydraulic resistance have a width of 20 μm, a depth of 20 μm, and a length of 7.5 mm; individual channels connect each emitter inlet to a common manifold pool through successive junctions forming a branched flow path.

The extractor, a 1mm thick Si wafer, is etched twice, first to carve an array of holes 0.9 mm in diameter and later up to 750 μm to accommodate the emitter. There is an extractor hole concentric to each emitter. A novelty of the source tested in this article is that the extractor electrode, the emitter electrode, and a glass wafer (used both for capping the common manifold pool and to serve as a surface supporting the electrodes) are joined together using anodic bonding. Figure 1 shows the integrated electrospray source.

Figure 2 illustrates the steps followed to assemble the source: the etched and cleaned emitter electrode and borofloat dice are aligned (1), put in contact and heated before imposing a voltage difference between them to form an anodic bonding at the contact interface (2). Then the cleaned dice with the extractor electrode (3) is aligned with the emitter dice and bonded to the borofloat substrate (4). The propellant is transferred to the microfluidic channels through a fused silica tube which is first glued to a fitting (5), which is in turned glued with epoxy to the borofloat (6).

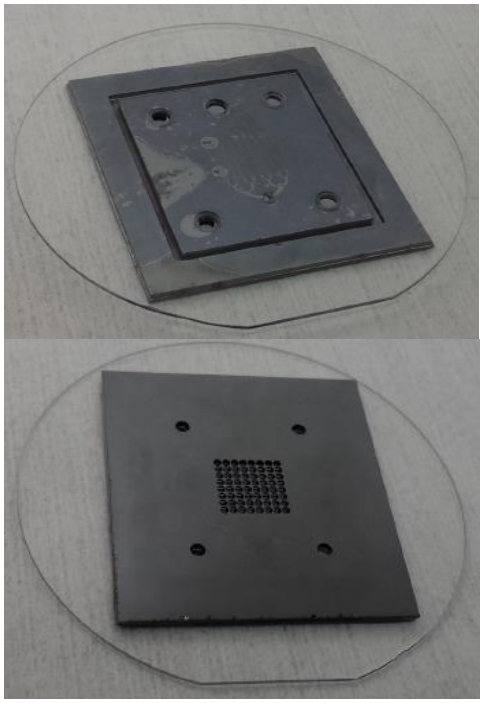

Figure 1. Integrated electrospray source. *The emitter and extractor electrodes are anodically bonded to a glass wafer that also works as the lid of the propellant manifold feeding the emitters.*

B. Experimental Set-up

Figure 3 shows a sketch of the experimental setup. The thruster head is mounted inside a vacuum chamber operated at a pressure below 10^{-5} Torr. Vacuum is provided by a turbomolecular pump backed by a mechanical forepump. The free end of the fused silica tube bonded to the glass wafer is submerged into the propellant, which is kept in a reservoir placed outside of the chamber. The pressure in this reservoir drives the desired propellant flow rate. The emitter array is connected to a high voltage source through a fast switch, used to interrupt the beam when measuring time-of-flight (TOF) waves. The voltage difference between the emitter and the grounded extractor will be referred to as the emitter potential, V_E. The particles in the beam and the associated current are intercepted by a collector electrode which, like the extractor, is at ground potential. The electric currents flowing into the emitter, extractor and collector electrodes are key variables for determining the performance of the source, and are measured with three electrometers integrated in the experimental set up. When measuring TOF waves the beam is directed to a special detector that can be inserted in the path of the beam with the help of a positioning stage. The collecting plate of this detector is shielded by an electron-suppressing screen biased at -10 V. The ionic liquid 1-ethyl-3-methylimidazolium bis(trifluoromethylsulfonyl) imide, EMI-Im is used as propellant.[16] The density, surface tension, viscosity, and electrical conductivity of EMI-Im at room temperature are 1520 kg/m^3, 0.0349 N/m, 0.034 Pa/s, and 0.88 S/m.

The TOF measurement resolves the populations of ions and charged droplets due to their very different charge to mass ratios, q/m, and therefore to their very different velocities, $v = \sqrt{2\,V_A\,q/m}$. V_A stands for the acceleration voltage, which is typically smaller than the emitter potential due to the dissipation of energy in the cone-jet, and the conversion of mechanical energy into surface energy. The energy loss can be

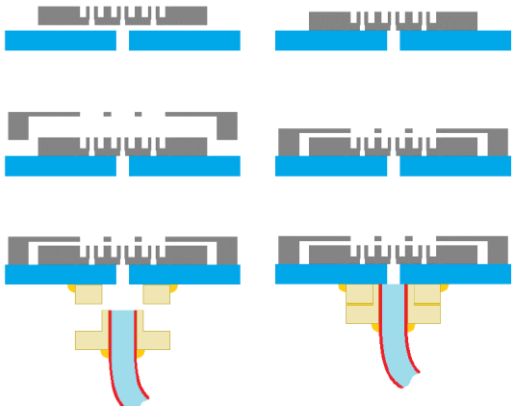

Figure 2. Steps in the assembly of the source.

expressed in terms of an average voltage loss, ϕ_L. The mass flow rate and thrust, key parameters in an electrospray thruster, can be obtained by integrating the time of flight signal $I(t)$:

$$\dot{m}_{TOF} = \int_0^\infty \frac{2 < V_A >}{L_{TOF}^2} t^2 I'(t)\, dt \tag{1}$$

$$T_{TOF} = \int_0^\infty \frac{2 < V_A >}{L_{TOF}} t\, I'(t)\, dt \tag{2}$$

where L_{TOF} is the distance between extractor and collector. Although the charged particles have a distribution of acceleration voltages, we use the average value $< V_A > = V_E - \phi_L$ because the distribution cannot be expressed as a function of the time of flight variable.

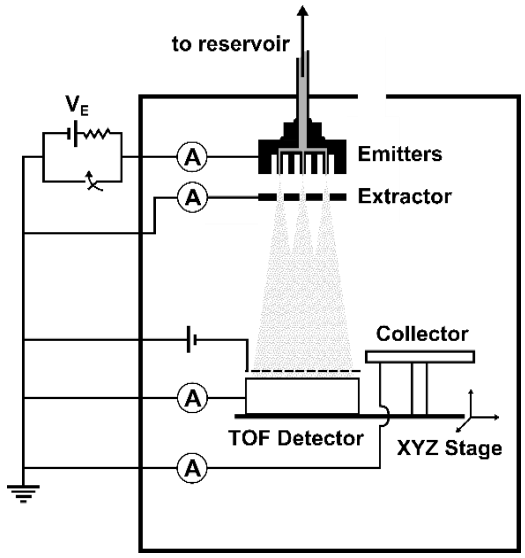

Figure 3. Experimental set-up.

C. Results

Figure 4 shows the current measured at the emitter electrode as function of the absolute pressure in the propellant reservoir, at intervals of 1 torr. The emitter potential is 1752 V. In this run we decrease the pressure very slowly (typically a torr within dozens of seconds), measure both the emitter current and the output of the pressure gauge multiple times, and record the average values. We also plot the standard deviation of the current points measured within 1-torr intervals, in the form of red vertical bars. Above 100 torr the standard deviations are very small, the I vs P curve is monotonic and follows the usual $I \propto Q^{1/2}$ law of cone-jets. The standard deviations at pressures below 100 torr are the largest, indicating that below this point the emission in some of the emitters is unstable (the flow of propellant at this point is not sufficient to have all emitters operating above the minimum flow rate at which the electrospray is stable). Although not shown in Figure 4, the current measured in the extractor was always a small fraction of the emitter current at all pressures.

Figure 5 shows time-of-flight curves for several beam currents. The voltage difference between the emitter and extractor is 1752 V. Before shorting the emitter to ground at $t = 0$, the beam is stationary and the current sensed by the TOF collector is constant over time; after the potential of the emitter is switched to ground at $t = 0$, suddenly interrupting the emission, the current sensed by the TOF collector decreases over time as the space between the extractor and the collector is emptied of charged particles; finally, because the particles in the beam have a distribution of velocities, the sensed current decreases to zero not as a sharp step, but in a smoother way reflecting the spread of velocities. The TOF technique easily resolves the ion and droplet populations in these beams because of their very different velocities. The TOF of the ions at all beam currents are very similar (although their *q/m* does not change with beam current, their acceleration voltages change slightly due to increasing voltage losses along the cone-jet at increasing beam current), while the average velocity of the droplets decreases substantially at increasing beam current (the average *q/m* of the droplets decreases with beam current).

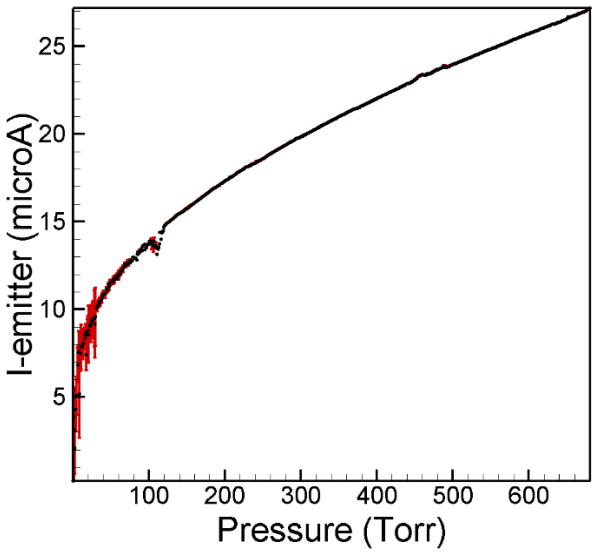

Figure 4. Emitter current as a function of the pressure of the propellant in the reservoir.

Table I lists the mass flow rate and thrust for the beams in Fig. 5 and for other similar pressures, together with the specific impulse and propulsive efficiency:

$$I_{sp} = \frac{T}{\dot{m} g_o} \quad (4)$$

$$\eta_p = \frac{T^2}{2\dot{m} I_B V_E} \quad (5)$$

Table I also lists the voltage loss, taken from measurements reported in reference [17]. We assume that all emitters yield the same current, $I_1 = I_E / 64$, to interpolate in the $\phi_L(I_1)$ experimental data. The mass flow rate and thrust divided by the number of emitters, and the specific impulse and propulsive efficiency, are similar to previous results obtained with a single emitter electrospraying EMI-Im.[4] The performance of the electrospray source is also very similar to the performance reported for a similar multiemitter source in which the extractor and emitter were not integrated.[15]

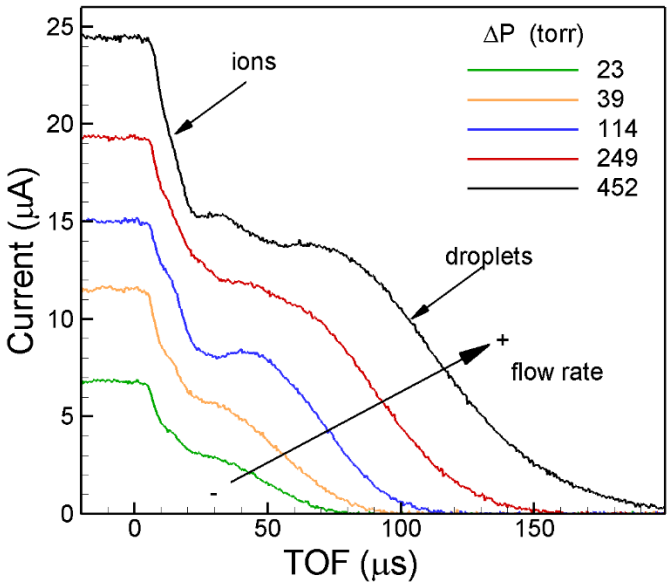

Figure 5. Time-of-flight measurements for several beam currents.

Table I. Pressure drop ΔP (Torr), emitter current I_E (μA), voltage loss ϕ_L (V), beam mass flow rate $\dot{m}_{TOF}$ (kg/s), thrust T_{TOF} (μN), specific impulse I_{sp} (s) and propulsive efficiency η_p calculated with the time-of-flight technique. The emitter potential is 1752 V.

ΔP	I_E	ϕ_L	$\dot{m}_{TOF}$	T_{TOF}	I_{sp}	η_p
23	6.82	91	$2.5 \cdot 10^{-9}$	5.9	242	59%
39	11.53	91	$6.0 \cdot 10^{-9}$	12.2	206	61%
83	13.7	107	$1.0 \cdot 10^{-8}$	17.6	179	64%
114	15.02	130	$1.3 \cdot 10^{-8}$	21.1	160	63%
174	16.98	165	$2.0 \cdot 10^{-8}$	27.3	139	63%
249	19.30	206	$2.9 \cdot 10^{-8}$	34.4	121	60%
305	20.87	227	$3.6 \cdot 10^{-8}$	39.2	112	58%
429	23.71	257	$4.9 \cdot 10^{-8}$	47.8	98	55%
452	24.42	263	$5.7 \cdot 10^{-8}$	51.5	92	54%

III. Conclusion

We have microfabricated and tested a 64-emitter electrospray source with all components (emitter and extractor electrodes, and a supporting glass wafer) bonded together. The main novelty of this design is the use of individual flow-restrictive channels for each emitter, etched on the back side of the emitter wafer. This method enables the independent implementation of emitter geometry and fluidics requirements. The electrospray source operates steadily in vacuum, with negligible interception of the beam by the extractor electrode. The source has been tested in a wide

range of flow rates. The time-of-flight technique was used to measure the mass flow rate, thrust, specific impulse and propulsive efficiency in the range of propellant reservoir pressures between 23 and 452 torr, and at constant emitter potential of 1752 V. The resulting thrust, specific impulse and efficiency ranged between 5.9 and 57 μN, 242 and 92 s, and 59% and 54 % with a maximum efficiency of 64%.

Acknowledgments

This work was funded by the U.S. Air Force Office of Scientific Research (AFOSR) grant no. FA9550-11-1-0308 and a Balsells Fellowship. The authors are grateful for the support of the AFOSR Program Manager Mitat Birkan, and of Pete Balsells and Roger Rangel (Balsells Foundation).

References

1 Beynon, J. C., Cohen, E., Goldin, D. S., Huberman, M. N., Kidd, P. W., and Zafran, S., "Present Status of Colloid Microthruster Technology", Journal of Spacecraft and Rockets, Vol. 5, No. 11, 1968, pp. 1319,1324.

2 Martinez-Sanchez, M., Fernandez de la Mora, J., Hruby, V., Gamero-Castaño, M., and Khayms, V., "Research on Colloid Thrusters", Proceedings of the 26th International Electric Propulsion Conference, IEPC Paper 99-014, Kitakyushu, Japan, 1999, pp. 93,100.

3 Mueller J., "Thruster Options for Microspacecraft: a Review and Evaluation of Existing Hardware and Emerging Technologies", 33rd Joint Propulsion Conference and Exhibit, Seattle, WA, AIAA Paper 97-3058, 1997.

4 Gamero-Castaño, M., and Hruby, V., "Electrospray as a Source of Nanoparticles for Efficient Colloid Thrusters". Journal of Propulsion and Power, Vol. 17, 2001, pp. 977,987.

5 Gamero-Castaño, M., "Energy Dissipation in Electrosprays and the Geometric Scaling of the Transition Region of Cone-Jets", Journal of Fluid Mechanics, Vol. 662, Nov. 2010, pp. 493-513.

6 Huberman M. N., and Rosen S. G., "Advanced High-Thrust Colloid Sources", Journal of Spacecraft and Rockets, Vol. 11, No. 7, 1974, pp. 475,480.

7 Ober, S., Branam, R., Huffman, R., Demmons, N., and Martin, R., "Electrospray Thruster for CubeSat", 49th AIAA Aerospace Sciences Meeting including the New Horizons Forum and Aerospace Exposition, Orlando, Florida, AIAA Paper 2011-522, 2011.

8 Lozano, P., and Martinez-Sanchez, M., "Ionic Liquid Ion Sources: Characterization of Externally Wetted Emitters", Journal of Colloid and Interface Science, Vol. 282, No. 2, 2005, pp. 415,421.

9 Legge R. S., and Lozano, P., "Electrospray Propulsion Based on Emitters Microfabricated in Porous Metals", Journal of Propulsion and Power, Vol. 27, No. 2, 2011, pp. 485,495.

10 Krpoun R., and Shea, H. R., "Integrated out-of-Plane Nanoelectrospray Thruster Arrays for Spacecraft Propulsion", Journal of Micromechanics and Microengineering, Vol. 19, No. 4, 2009, 045019.

11 Krpoun, R., Smith, K. L., Stark, J. P. W., and Shea, H. R., "Tailoring the Hydraulic Impedance of out-of-Plane Micromachined Electrospray Sources with Integrated Electrodes", Applied Physics Letters, Vol. 94, No. 16, 2009, 163502.

12 Lenguito, G., Fernandez de la Mora, J., and Gomez, A., "Scaling up the Power of an Electrospray Microthruster", Journal of Micromechanics and Microengineering, Vol. 24, No. 5, 2014, 055003.

13 Krpoun, R., "Micromachined Electrospray Thrusters for Spacecraft Propulsion", Doctoral dissertation, École Polytechnique Fédérale de Lausanne, 2009.

14 Dandavino, S., Ataman, Ç., Ryan, C., Chakraborty, S., Courtney, D. G., Stark, J. P. W., and Shea, H. R., "Microfabricated Electrospray Emitter Arrays with Integrated Extractor and Accelerator Electrodes for the Propulsion of Small Spacecraft", Journal of Micromechanics and Microengineering, Vol. 24, No. 7, 2014, 075011.

15 Grustan-Gutierrez, E., and Gamero-Castaño, M., "Microfabricated electrospray thruster array with high hydraulic resistance channels", Journal of Propulsion and Power, Vol. 33, 2017, pp. 984, 991.

16 A. B. McEwen, H. L. Ngo, K. LeCompte, J. L. Goldman. Electrochemical Properties of Imidazolium Salt Electrolytes for Electrochemical Capacitor Applications. J. Electrochem. Soc. 146, 199, pp. 1687,1695.

17 Gamero-Castaño, M., "Characterization of the electrosprays of 1-Ethyl-3-Methylimidazolium Bis(Trifluoromethylsulfonyl) Imide in vacuum", Physics of Fluids, Vol. 20, 2008, 032103.